

A Sea of Black Holes: Characterizing the LISA Signature for Stellar-Origin Black Hole Binaries

KRYSTAL RUIZ-ROCHA,¹ KELLY HOLLEY-BOCKELMANN,^{1,2} KARAN JANI,¹ MICHELA MAPELLI,^{3,4,5} SAMUEL DUNHAM,⁶ AND WILLIAM GABELLA¹

¹*Department of Physics and Astronomy, Vanderbilt University, Nashville, TN 37235, USA*

²*Department of Life and Physical Sciences, Fisk University*

³*Institut für Theoretische Astrophysik, ZAH, Universität Heidelberg, Albert-Ueberle-Straße 2, D-69120, Heidelberg, Germany*

⁴*Physics and Astronomy Department Galileo Galilei, University of Padova, Vicolo dell'Osservatorio 3, I-35122, Padova, Italy*

⁵*INFN - Padova, Via Marzolo 8, I-35131 Padova, Italy*

⁶*TAPIR, Mailcode 350-17, California Institute of Technology, 1200 E California Blvd, Pasadena, CA 91125, USA*

ABSTRACT

Observations by the LIGO, Virgo and KAGRA (LVK) detectors have provided new insights in the demographics of stellar-origin black hole binaries (sBHB). A few years before gravitational-wave signals from sBHB mergers are recorded in the LVK detectors, their early coalescence will leave a unique signature in the ESA/NASA mission Laser Interferometer Space Antenna (LISA). Multiband observations of sBHB sources between LISA and LVK detectors opens an unprecedented opportunity to investigate the astrophysical environment and multi-messenger early-alerts. In this study, we report the sBHB sources that will be present in the LISA data derived directly from the hydrodynamic cosmological simulation Illustris. By surveying snapshots across cosmological volume, metallicity and look-back time, we find that about tens to thousand sBHB candidates will be present in the LISA data for various combinations of mission lifetime. For estimates consistent with the LVK rates, we find that only 20 sBHBs across Illustris snapshots will be detected with significant confidence for a 10-year LISA mission, while a 4-year LISA mission would detect only 2 sBHBs. Our work paves the way for creating LISA mock data and bench marking LISA detection pipelines directly using cosmological simulations.

Keywords: gravitational waves—stars:black holes—multimessenger astronomy—LISA

1. INTRODUCTION

The Laser Interferometer Gravitational-Wave Observatory (LIGO) made the first direct detection of gravitational waves in 2015, revealing a merger of black holes with masses 36 and 29 M_{\odot} (Abbott et al. 2016). These black holes, dubbed *stellar origin binary black holes* (sBHB) by the gravitational wave community, are much more massive than the roughly 10 M_{\odot} black holes in accreting binaries that had been detected electromagnetically (van den Heuvel 2019). This discovery expanded our understanding of black hole populations, providing insight into their formation and evolution (Abbott et al. 2016a,b). However, the formation channel of these binaries is still under debate. The current favored mechanisms involve formation via: a) isolated binaries in the galactic field (Bethe & Brown 1998; Belczynski et al. 2002; Banerjee et al. 2010; Mennekens & Vanbeveren 2014; Belczynski et al. 2016; de Mink & Mandel 2016; Marchant et al. 2016; Giacobbo et al. 2018; Kruckow et al. 2018) ; b) dynamical interactions within dense stellar

environments (Portegies Zwart & McMillan 2000; Banerjee et al. 2010; Ziosi et al. 2014; Rodriguez et al. 2015, 2016; Mapelli 2016; Banerjee 2017; Askar et al. 2017; Rodriguez et al. 2021); and c) binaries within gaseous AGN accretion disks (McKernan et al. 2018; Stone et al. 2017; Bartos et al. 2017; Ford & McKernan 2022).

sBHBs are so massive that they are a new source class for the Laser Interferometer Space Antenna (LISA), an ESA/NASA space-based gravitational wave observatory set to launch in 2035 (Amaro-Seoane et al. 2017a; Colpi et al. 2024). LISA is sensitive from around 10^{-4} to 0.1 Hz, a frequency range that captures the inspiral phase of the sBHB population. In the LISA band, low frequency sBHBs are relatively widely-separated, take millions of years to merge, and may generate an unresolved stochastic background (Babak et al. 2023). The higher frequency sources are more tightly-bound, sweeping through the LISA band in the last phase of inspiral months to days before merging within ground-based gravitational wave

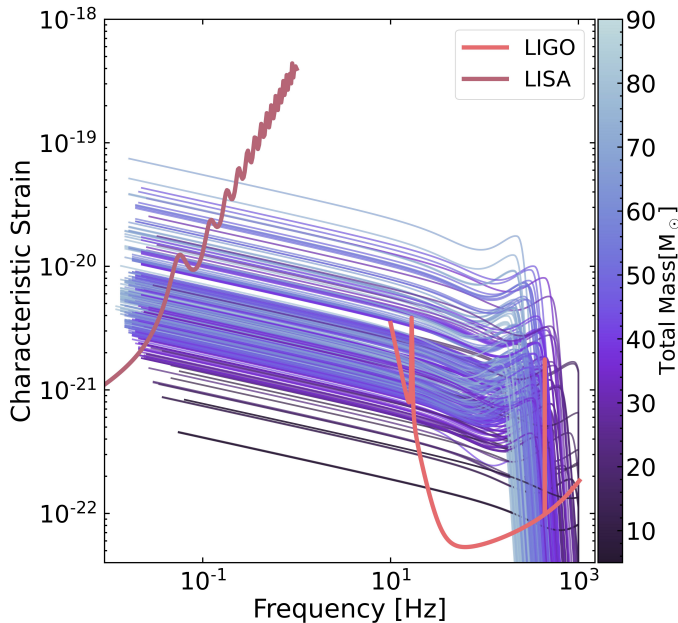


Figure 1. Characteristic strain versus frequency for sBHBs formed within the oldest snapshot of the Illustris-1 simulation at redshift $z=13.4$ (Mapelli et al. 2017). We only show a subset of these sBHBs that eventually merged under $z \leq 0.5$. The strain from each sBHB is colored by the total binary mass in the source frame. The left curve line is LISA’s sensitivity curve, the right curve is LIGO’s sensitivity curve.

detectors, making them a prime multiband source (Sesana 2016; Cutler et al. 2019; Jani et al. 2020).

Multiband observations alone enable a more accurate measurement of masses, spins, eccentricity, and distance (Vitale 2016; Randall & Xianyu 2021; Toubiana et al. 2021; Ranjan et al. 2024), but their unique power is in providing better spatial resolution and enough lead time before merger to conduct rigorous observational campaigns to identify electromagnetic counterparts (Baker et al. 2019; Lamberts et al. 2019; Korol et al. 2017; Digman & Cornish 2023). Multiband data is vital to differentiate between sBHB formation channels as well as to constrain their final evolutionary sequence (Breivik et al. 2016; Baker et al. 2019; Amaro-Seoane et al. 2017b).

To investigate the possibility that stellar origin binaries arise in an isolated binary stellar population, Mapelli et al. (2017) used the cosmological hydrodynamic simulation suite Illustris (Vogelsberger et al. 2014a) to predict the astrophysical and LIGO-observable rate of sBHB mergers, given a range of binary stellar population models. Illustris provided a self-consistent time-evolving map of star-formation rate, mass, and metallicity to be used as input to a

binary population synthesis code, making it possible to paint a stellar population onto the simulation, let it evolve, and track the formation and ultimate merger of sBHBs.

Our work extends this study, identifying those sBHB mergers within the Illustris simulation volume that are observable with LISA. Formally, the time to merge for sBHBs in the LISA band can be from months to millions of years, but we narrowed our investigation to those sBHBs that transition from LISA to ground-based detectors within the lifetime of the LISA mission; these sources are the loudest in the LISA band and are therefore the most promising for multiband and multi-messenger observations (Gerosa et al. 2019). Figure 1 is a subset of sBHB mergers within the Mapelli et al. (2017) database that may be seen by LISA and merge within LIGO. These binaries are chosen from the snapshot at the highest redshift ($z = 13.4$), because it contains sBHBs that merge within a wide variety of lookback times, showing the robustness of Mapelli et al. (2017)’s database for studying multi-messenger astronomy.

The paper proceeds as follows: Section 2 describes our methods, including a brief review of the simulation, the stellar population input from Mapelli et al. (2017). In addition, section 2.1 discusses the signal-to-noise calculations for our binary database. In section 3 we discuss the results, including the multiband rates (section 3.1), and number of detectable multiband sources (section 3.2). Finally, the conclusion and discussion are within section 4 where we summarize our results, point out caveats, and identify areas for future work.

2. METHODS

Illustris is a set of cosmological hydrodynamic N-body simulations run using the AREPO moving mesh code (Vogelsberger et al. 2014a; Springel 2010). To model galaxy formation and evolution in a cosmological context, the simulation self-consistently treats dark matter, supermassive black holes, gas, and stars, including prescriptions for gas cooling, star formation, metal enrichment, supernovae and associated feedback, as well as massive black hole formation and evolution (including gas accretion, mergers, and several modes of feedback). Illustris is a cosmological volume of 106.5^3 Mpc^3 initialized in a Wilkinson Microwave Anisotropy Probe (WMAP-9) cosmology with the following parameters (Hinshaw et al. 2013): $\Omega_M = 0.2726$, $\Omega_\Lambda = 0.7274$, $\Omega_b = 0.0456$, $h = 0.704$, and $H_0 = 70.4 \text{ kms}^{-1}\text{Mpc}^{-1}$, where Ω represents the mean density relative to the critical

density of the Universe, and M , Λ , and b refer to matter, the cosmological constant, and baryons, respectively. h is the dimensionless Hubble parameter (Croton 2013), and H_0 the Hubble constant. The Illustris suite is composed of 6 simulations: ILLUSTRIS-(1,2,3), which are the hydrodynamical simulations modeling galaxy formation and include all the star formation, gas and massive black hole physics described above, and ILLUSTRIS-DM-(1,2,3), which are the dark matter-only variant. We use Illustris-1 for its higher mass resolution; the Illustris-1 simulation contains 1.6×10^{12} particles over all snapshots, with a dark matter mass resolution of $6.3 \times 10^6 M_\odot$, a baryonic matter mass resolution of $1.3 \times 10^6 M_\odot$ and a softening length of ~ 710 pc for stars and supermassive black holes (SMBHs) (Vogelsberger et al. 2014a,b).

Although the Illustris simulation suite is state-of-the-art, it cannot resolve individual stars and stellar remnants. Therefore, Mapelli et al. (2017) maps a population of sBHB, each stellar particle in snapshots spanning redshifts 0–16 using an updated version of the public binary stellar population synthesis code, Binary Star Evolution (BSE) (Hurley et al. 2000, 2002) called MOBSE (Giacobbo et al. 2018). For more detail about the procedure to seed Illustris with sBHB, please see Mapelli et al. (2017); we briefly describe the process here. Mapelli et al. (2017) constructed a library of 72 distinct binary stellar population models, each ‘book’ in the library consisting of millions of sBHBs representing a particular metallicity and a set of assumptions about the less well-constrained binary-evolution physics, such as mass loss in the common-envelope phase.

Using this library, a sBHB distribution is assigned to Illustris-1 star particles. The metallicity of a star particle determines which stellar population ‘book’ to use, and the mass of the star particle determines how many sBHB to select. Each sBHB is characterized by its masses, separation, and eccentricity, which is used to calculate the binary merger timescale. By following only the sBHB that merge within a Hubble time, this earlier work resulted in a simulated census of the astrophysical merger rates for these sources, as well as estimates of the number of binaries and mass distribution of sBHB mergers that LIGO will see for various stellar population models, as shown in Figure 6 of Mapelli et al. (2017).

Note that for our paper, we adopt models D and DK as our fiducials; these assume a delayed supernova model, a treatment of Hertzsprung gap (HG) donors, and natal kicks for compact binaries (Mapelli et al. 2017). The difference between model D and DK is that D employs

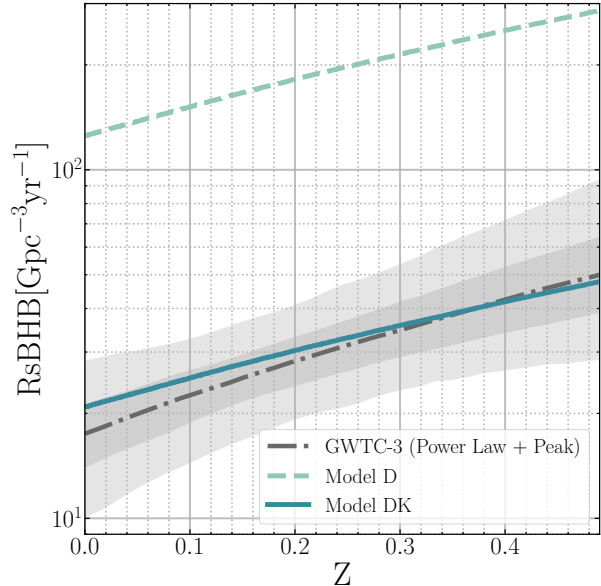


Figure 2. Rate versus redshift for the fiducial model D and DK. The dotted grey line and contours are a reproduction of LIGO’S O3 rate from Abbott et al. (2023a)

a method described in Fryer et al. (2012) to rescale natal kicks for black holes to take into account the fraction of the stellar envelope that can fall back onto the compact object during the explosion, f_b , which can range from 0 to 1 (Fryer et al. 2012; Spera et al. 2015), as shown by equation 1

$$v_{BH} = v_{NS}(1 - f_b), \quad (1)$$

where v_{NS} is the velocity distribution in (Hobbs et al. 2005). Model DK applies the velocity distribution found by Hobbs et al. (2005) for natal kicks of neutron stars to the black holes.

The sBHB merger rate in model D is $181 \text{ Gpc}^{-3} \text{ yr}^{-1}$ at a redshift of 0.2. At the time of publication, this rate was the most consistent with O1 LIGO observations. However, LIGO data from its observing run 3 (O3) places the sBHB merger rate between 17.9 and $44 \text{ Gpc}^{-3} \text{ yr}^{-1}$ at a redshift of 0.2 (Abbott et al. 2023a). This filters into our results as an overestimate of the LISA and LIGO multiband rate when we use model D. In contrast, model DK offers a much closer match to O3 rates with a sBHB merger rate of $29 \text{ Gpc}^{-3} \text{ yr}^{-1}$ at redshift 0.2. This similarity is shown in Figure 2 which plots the merger rates for model D, DK, and LIGO’S rate for O3 against redshift. The dashed line represents model D’s rate and the lower line is model DK’s rate. LIGO’s rate is shown by the dotted gray line with the inner contours containing 50% of the data and the outer contours containing 90% of the data. Model DK’s rate consistently falls within the 50% contours across the full redshift range and

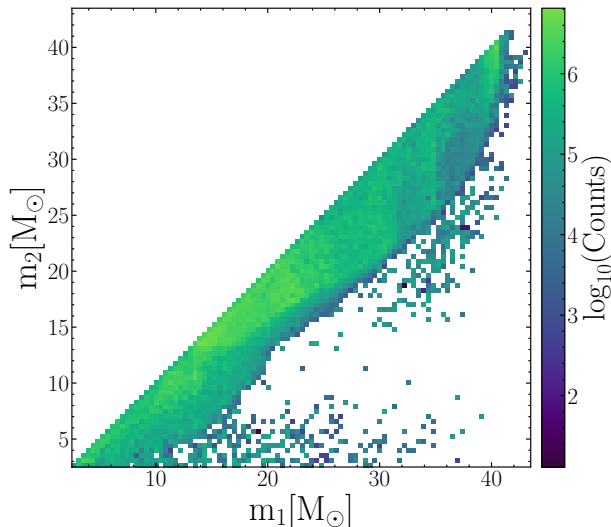


Figure 3. Heatmap of BHB mass distribution for first BH mass (m_1) and second BH mass (m_2) for the Mapelli post-processing files restricted to a sBHBs merging below redshift 0.5. The original database did not have m_1 always greater than m_2 . However within this figure we set m_1 to be greater than m_2 for all sBHBs. The colors represent the log of the counts of the sBHBs in each bin.

aligns more closely to LIGO’s rate for $z > 0.3$. We note that the star formation rate history in the ILLUSTRIS-1 simulation is overall in good agreement with observations (Madau & Fragos 2017), except for an overestimate of $\sim 40\%$ at low redshift ($z \lesssim 0.2$). However, this overestimate has a negligible impact on the merger rate density of sBHBs (Mapelli et al. 2017), because only stars with nearly solar metallicity form at such a low redshift: the efficiency of BHB mergers drops by about three orders of magnitude if the metallicity Z is $> 0.2 Z_\odot$ (Giacobbo et al. 2018).

2.1. Calculating the Signal-to-Noise Ratio in the LISA Band

We began with 108 snapshots ranging from redshift 0.0072 to 13.6, each consisting of a database of the sBHB formed at that redshift. This database contains information on: 1. the progenitor stellar particle ID from Illustris; 2. metallicity; 3. black hole component masses; 4. formation redshift; 5. sBHB merger time.

Since each snapshot contains only those sBHB that formed within a particular snapshot time interval, the varying sBHB merger time implies that a sBHB at a previous snapshot may still exist at a given redshift, but will be missing in the snapshot; indeed, the sBHBs seeded in a given snapshot will merge in the future over a wide range of timescales. It is worth reiterating that the database only contains sBHBs that merge within a Hubble time. Consequently, sBHBs in the simulated

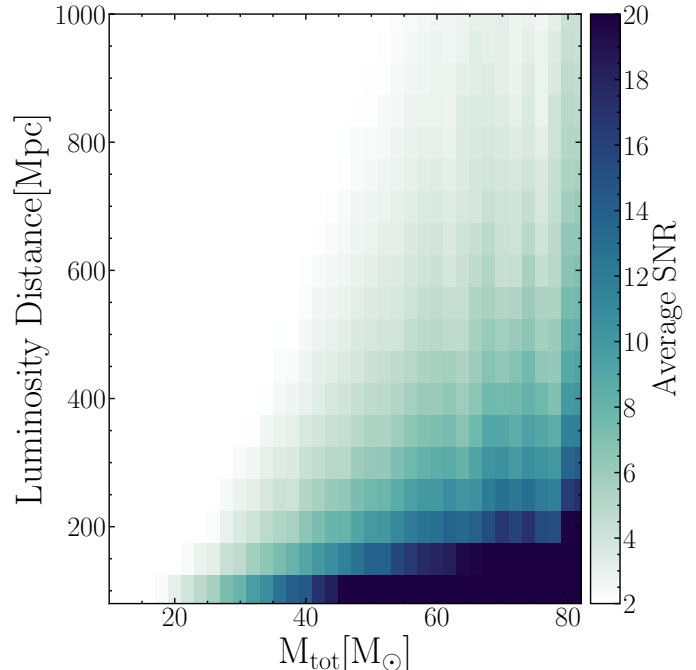


Figure 4. Heatmap of the total mass and luminosity distance colored by the average SNR in each grid for a LISA mission lifetime of 10 years.

population that do not merge by the present day are missing from the current database. We leave the analysis of the quasi-static sBHB population for a future paper.

To identify sBHB mergers that will be observable by both LISA and LIGO, we first restrict the database to those sBHBs that merge within a horizon redshift of 0.5; this decision greatly reduced the number of sBHBs in the Illustris volume from 7.7×10^9 to 1.19×10^9 . Our choice is conservative and encompasses the expected horizon distance for sBHBs (see Figure 2 of Jani et al. (2020)). Figure 3 displays the black hole mass distribution for those systems that merge within a Hubble time and merge below a redshift of 0.5 in model D. We also forced the m_1 to always be greater than m_2 , which was not the case in our database. In these models, the most common sBHB merger arises between black holes with commensurate masses of roughly $15\text{--}25 M_\odot$. We caution that neither model D nor DK contain sBHBs with component masses $m_{\text{BH}} > 43 M_\odot$. LIGO has certainly observed black holes more massive than the upper limit of these models (Abbott et al. 2019, 2021, 2023b, 2024). It may well be that the high mass end of the observed BHB merger mass spectrum represents additional processes, such as hierarchical merging, that may be at play and are therefore not well-represented by BSE (Hurley et al. 2000, 2002; Giacobbo et al. 2018). We leave a

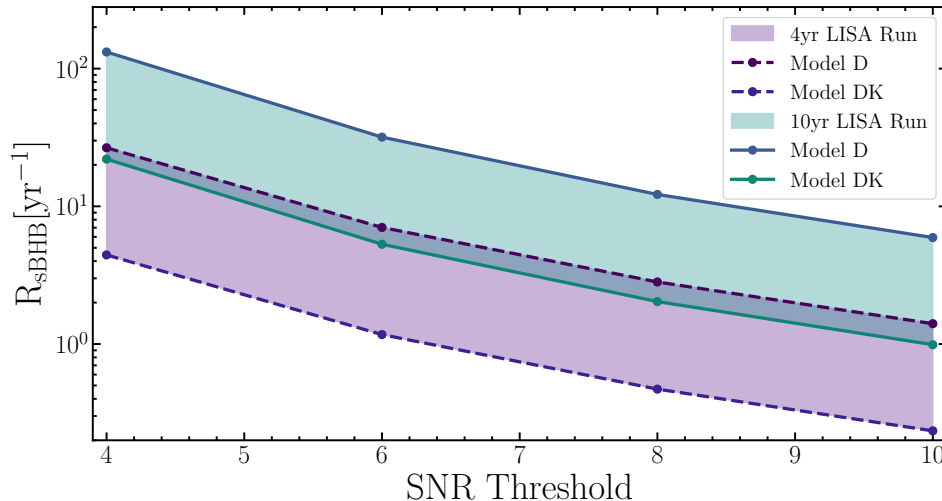


Figure 5. Multiband rates calculated for our sBHBs database using equation 3 for both Model D and Model DK for a 4-year LISA mission, shown with purple contours, and a 10-year LISA mission shown with the teal contours.

multiband treatment of the higher mass black holes observed by LIGO to a future paper.

Using the redshift-limited database, we extract the masses and lookback time for each black hole binary merger and determine the gravitational wave frequency, f_{obs} , of these binaries at a time T_{obs} before the merger, using:

$$f_{\text{obs}} = \frac{c^3}{8\pi GM_c} \left(\frac{5GM_c}{c^3} \right)^{3/8} \frac{1}{T_{\text{obs}}^{3/8}}, \quad (2)$$

where c is the speed of light, G is the gravitational constant, M_c is the chirp mass, and T_{obs} is the time until the BHB merges in seconds (Chan et al. 2018; Bassan 2014). We adopt 4 and 10 years for T_{obs} , the projected duration of science operations for the LISA mission. As outlined in Gerosa et al. (2019), this choice produces a louder SNR in the LISA band while enabling a relatively contemporaneous multiband source. (Gerosa et al. (2019) considered a T_{wait} , the time between detecting an event with a space-based and a ground-based detector. In our work, T_{obs} is the same as T_{wait} .) The masses in equation 2 are in the detector frame, and are converted from the source frame found in the database to detector frame masses using: $m_{\text{detector}} = m_{\text{source}}(1+z)$, where z is the sBHB merger redshift.

3. RESULTS

3.1. Multiband Rate for detectable sBHBs

With this information we can then calculate the signal-to-noise ratio (SNR). For this, we use the python LISA Sensitivity package given an observation duration and cosmology (Robson et al. 2019). This code models

LISA’s sensitivity to laser shot noise, acceleration noise, and test-mass force noise over a mission duration, and calculates the characteristic strain, and SNR of a binary given the component masses, distance, and an optional sky location and inclination. Note that unless specified, the SNR is averaged over inclination angle, polarization, and sky position. Additionally, since the sBHBs did not include spin, the gravitational wave signal is approximated by a phenomenological waveform model for non-spinning binaries, referred to as PhenomA (Ajith et al. 2007). In the database, the LISA SNR for a observation run of 10 years technically ranged from 0 to 1×10^7 , with the anomalously high SNR populated by a sBHB at a luminosity distance of less than a kpc. Figure 4 maps the average SNR as a function of total mass and luminosity distance assuming a mission duration of 10 years. In this figure we see, as expected, that nearby high mass binaries yield the highest SNR. For example sBHB system with $M_{\text{tot}} = 80 M_{\odot}$ will be visible up to 200 Mpc in LISA with $\text{SNR} \gtrsim 20$. Such high-mass binaries will be visible in LISA out to ~ 1 Gpc with an average SNR ~ 6 .

The luminosity distance for high-mass sBHB in Figure 4 at a SNR threshold of 8 is consistent with the multiband detection radius reported in Jani et al. (2020).

Now that we have the SNR for each sBHB in hand, we can determine the multiband event rates and the expected number of detections for LIGO and LISA as a function of SNR.

We calculate the expected astrophysical rate of a population above a certain SNR threshold using

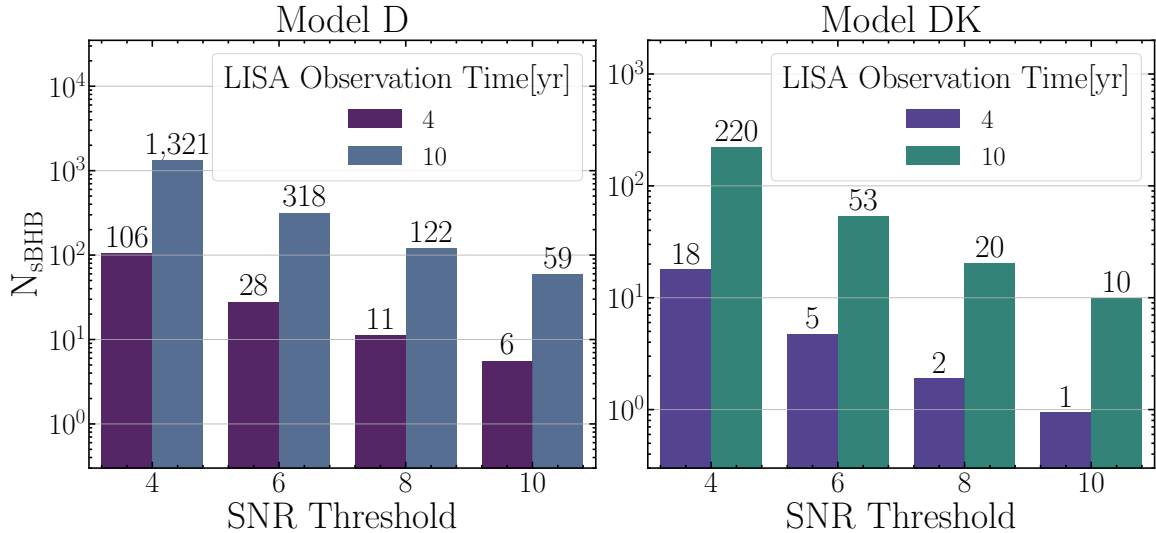


Figure 6. The expected number of multiband sBHBs calculated for different SNR thresholds. The left panel assumes model D and a 4 or 10-year LISA mission, while the right panel model assumes model DK, which better approximates the O3 LIGO event rate.

equation 3 from (Chen et al. 2022):

$$\frac{dN}{dzdt} = \frac{d^2n(z)}{dzdV_c} \frac{dz}{dt} \frac{dV_c}{dz} \frac{1}{1+z}, \quad (3)$$

where V_c is the co-moving volume, $n(z)$ is the number of sBHBs at a redshift z , $\frac{1}{1+z}$ converts $\frac{dz}{dt}$ to the observer frame, and $\frac{d^2n(z)}{dzdV_c}$ is the rate found in the simulation volume above a certain SNR threshold. This can be found directly from the simulation, expressed by:

$$\frac{d^2n(z)}{dzdV_c} = \frac{N(z)}{\Delta z V_{sim}}, \quad (4)$$

where $N(z)$ is the number of sBHBs merging within a redshift bin, Δz is the width of the redshift bin and V_{sim} is the simulation volume, which in our case is $(106.5\text{Mpc})^3$.

The multiband rate of sBHB mergers as a function of SNR is shown in Figure 5 for 4-year (purple) and 10-year (teal) LISA mission for model D and model DK.

During a 4-year observational run, our results for model D indicate that LISA and LIGO will detect 27 sBHBs yr^{-1} with $\text{SNR} \geq 4$. However, this number drops to 2 yr^{-1} when we increase the SNR threshold to 10 for model D. Model DK also shows the same pattern but is six times smaller than model D, i.e 5 yr^{-1} for $\text{SNR} \geq 4$ to 0.3 yr^{-1} for an $\text{SNR} \geq 10$.

If we extend the observational run to 10 years, the detectable multiband rate increases to 132 yr^{-1} with an SNR threshold of 4 to 6 yr^{-1} for $\text{SNR} \geq 10$. For model DK we see only 22 yr^{-1} for $\text{SNR} \geq 4$ to 1 yr^{-1} for $\text{SNR} \geq 10$.

3.2. Expected Number of Multiband sBHBs

Converting the multiband rate from equation 4 to the number of detectable sBHBs, we used:

$$N = \frac{dN}{dzdt} T_{\text{obs}}, \quad (5)$$

where $\frac{dN}{dzdt}$ is the rate from equation 4 and T_{obs} is the LISA mission lifetime. Figure 6 displays the number of sBHB that can be detected by both LIGO and LISA given a 4- and 10-year LISA mission lifetime. We see once again that the detectable multiband BH rate decreases as the SNR thresholds increase for both a 4-year and 10-year mission. For a 4-year LISA run, model D (left panel) exhibits a detectable number of multiband sBHB mergers that ranges from 6–106 as the SNR threshold decreases from 10 to 4, while model DK (right panel) yields between 1–18. For a 10-year mission, the number of sBHB mergers in model D ranges from 59–1321, and from 10–220 for model DK.

From our results, we conclude that the multiband detection rates (per year) for a 10-year LISA mission increases by $\sim 4x$ for both the models across all SNR thresholds when compared to a 4-year LISA mission. This is consistent with an average increase in SNR of sBHB by around $\sqrt{10/4}$ between the two LISA mission lifetimes, thus increasing the detection volume by a factor of ~ 4 . Similarly, the total number of multiband detections in a 10-year LISA mission is $\sim 10x$ higher at SNR threshold of 10 and $\sim 12x$ higher at SNR threshold of 4 when compared to 4-year LISA mission. The mild increase at low SNR thresholds compared to high SNR thresholds is due to an increase in the

intrinsic sBHB merger rates with redshift in the local universe (Mapelli et al. 2017).

3.3. Comparison to Previous Work

Previous work has been done to estimate sBHB multiband rates and expected numbers for LISA (Gerosa et al. 2019; Sesana 2016, 2017; Kyutoku & Seto 2016; Zhao et al. 2023). Sesana (2016, 2017) presented a semi-analytic data-driven approach using LIGO observations from O1, assuming two underlying black hole mass distributions and intrinsic merger rates: a Salpeter mass function with a merger rate of $100 \text{ Gpc}^{-3}\text{yr}^{-1}$, and log-uniform mass function with a rate of $35 \text{ Gpc}^{-3}\text{yr}^{-1}$. These higher merger rates inferred from O1 naturally lead to a larger number of predicted multiband events compared to our models.

Kyutoku & Seto (2016) examined the multiband detection of GW150914-analogs assuming an O1 event rate as well, however this work was primarily focused comparing the effect of different noise curves for eLISA, a precursor to the mission architecture adopted by LISA. For a 10 year mission, they predicted that the number eLISA-LIGO multiband sBHB detections ranged from 8–400, depending on the mission configuration.

Gerosa et al. (2019) updated the data-driven approach of the Sesana work using LIGO/Virgo/KAGRA observations from O1 and O2; the Salpeter mass function yielded a merger rate of $57_{-25}^{+40} \text{ Gpc}^{-3}\text{yr}^{-1}$, while the log-uniform yielded a rate of $19_{-8.2}^{+13} \text{ Gpc}^{-3}\text{yr}^{-1}$. For a 10-year LISA mission, their finding of 4-22 multiband LISA+LVK detections above an SNR of 8 is most consistent with our model DK, while model D is roughly 6 times higher.

Additionally, Gerosa et al. (2019) created binary population synthesis simulations with spinning black hole binaries for isolated systems that evolved through the common-envelope phase. They perform multiple models, each varying the natal kicks distributed using a Maxwellian distribution with a dispersion between 0 and 265 km/s, and noted that the expected multiband detection rates can vary by more than an order of magnitude depending on the natal kick choice, consistent with our findings.

Zhao et al. (2023) created a Monte Carlo-sampled database of mock sBHB based on GWTC-3 observations with a rate of $19_{-8.5}^{+8.4} \text{ Gpc}^{-3}\text{yr}^{-1}$. For a 4-year LISA mission and an SNR threshold of 8 they predict 3-15 events, which falls within the range of both of our models.

4. CONCLUSION

In this paper, we aimed to predict the expected rate and signature of stellar origin binary black holes that will be detectable by both LISA and LVK, with the hope that the early warning of a merger will help constrain sky location and help facilitate an alert of an impending merger for electromagnetic and ground-based GW detectors. Combining two binary population synthesis models with a cosmological hydrodynamic simulation, we found the multiband rate and expected number of sBHB detectable as a function of SNR and LISA mission duration. Table 1 summarizes our findings for four different mission durations. In this table, we define marginal detections as those with $\text{SNR} \geq 4$, while confirmed sBHB detections must have $\text{SNR} \geq 8$. Model DK produces the minimum value in each column while model D yields the maximum value. We note that model DK, the binary population synthesis model with larger supernova natal kicks, yields overall sBHB merger rates that are more consistent with LVK observations through O3. Although it may be tempting to conclude that small black hole natal kicks can be ruled out by LVK observations, the number of competing open questions in binary stellar evolution – from the strength of core overshooting, to the impact of unstable mass transfer, to the core-collapse explosion process itself – preclude the ability to do so. Advances in binary stellar population modeling will allow a better mapping of the unknown parameter space in binary stellar evolution and will therefore better enable comparisons to gravitational wave observations (Spera et al. 2019).

Our work provides a novel approach for building LISA mock data catalogs of sBHB directly using cosmological simulations. Such synthetic catalogs provide useful benchmark for LISA data-analysis pipelines (Babak et al. 2010; Baghi 2022; Lackeos et al. 2023). To maximize the LISA SNR of a given sBHB, we deliberately modeled those that would merge over a timescale that is roughly the LISA mission duration; there are certainly sBHBs that will merge in a ground-based gravitational wave band hundreds of years in the future, but these sources are much fainter in the LISA band when so far from merger, and are therefore not ideal multiband sources. We also neglected sBHBs that did not merge by the end of the simulation; this population of monochromatic, or nearly monochromatic, sBHBs may well be buried in the confusion foreground of Galactic compact object binaries (Colpi et al. 2024).

This study considers only the field sBHB formation channel, yet LVK observations may hint that multiple

Table 1. Expected number of multiband sBHBs for a range of LISA mission durations. The terms marginal and expected are defined by $\text{SNR} \geq 4$ and $\text{SNR} \geq 8$, respectively. For each range, the lower value represents model DK, while the higher value represents model D.

LISA mission lifetime	Marginal sBHB detections	Confirmed sBHB detections
4 years	18 – 106	2 – 11
6 years	53 – 320	5 – 32
8 years	118 – 708	11 – 68
10 years	220 – 1321	20 – 112

formation channels could be at play (Bouffanais et al. 2021). Cosmological simulations of the scale needed to make universal predictions are as yet unable to resolve AGN disks and dense stellar systems such as nuclear star clusters and globular clusters. We will explore building a framework to seed a simulation with sBHB from multiple formation channels in a future work.

ACKNOWLEDGMENTS

KHB acknowledges and appreciates support from NSF NRT-2125764. M.M. acknowledges financial

support from the European Research Council for the ERC Consolidator grant DEMOBLACK, under contract No. 770017 (PI: Mapelli) and from the German Excellence Strategy via the Heidelberg Cluster of Excellence (EXC 2181 - 390900948) STRUCTURES. This work used the resources provided by the Vanderbilt Advanced Computing Center for Research and Education (ACCRE), a collaboratory operated by and for Vanderbilt faculty at Vanderbilt University.

REFERENCES

- Abbott, B. P., Abbott, R., Abbott, T. D., et al. 2016, *Phys. Rev. Lett.*, 116, 061102, doi: [10.1103/PhysRevLett.116.061102](https://doi.org/10.1103/PhysRevLett.116.061102)
- Abbott, B. P., Abbott, R., Abbott, T. D., et al. 2016a, *ApJL*, 818, L22, doi: [10.3847/2041-8205/818/2/L22](https://doi.org/10.3847/2041-8205/818/2/L22)
- . 2016b, *PhRvL*, 116, 061102, doi: [10.1103/PhysRevLett.116.061102](https://doi.org/10.1103/PhysRevLett.116.061102)
- . 2019, *Physical Review X*, 9, 031040, doi: [10.1103/PhysRevX.9.031040](https://doi.org/10.1103/PhysRevX.9.031040)
- Abbott, R., Abbott, T. D., Abraham, S., et al. 2021, *Physical Review X*, 11, 021053, doi: [10.1103/PhysRevX.11.021053](https://doi.org/10.1103/PhysRevX.11.021053)
- Abbott, R., Abbott, T. D., Acernese, F., et al. 2023a, *Physical Review X*, 13, 011048, doi: [10.1103/PhysRevX.13.011048](https://doi.org/10.1103/PhysRevX.13.011048)
- . 2023b, *Physical Review X*, 13, 041039, doi: [10.1103/PhysRevX.13.041039](https://doi.org/10.1103/PhysRevX.13.041039)
- . 2024, *PhRvD*, 109, 022001, doi: [10.1103/PhysRevD.109.022001](https://doi.org/10.1103/PhysRevD.109.022001)
- Ajith, P., Babak, S., Chen, Y., et al. 2007, *Classical and Quantum Gravity*, 24, S689, doi: [10.1088/0264-9381/24/19/S31](https://doi.org/10.1088/0264-9381/24/19/S31)
- Amaro-Seoane, P., Audley, H., Babak, S., et al. 2017a, arXiv e-prints, arXiv:1702.00786, <https://arxiv.org/abs/1702.00786>
- . 2017b, arXiv e-prints, arXiv:1702.00786, <https://arxiv.org/abs/1702.00786>
- Askar, A., Szkudlarek, M., Gondek-Rosińska, D., Giersz, M., & Bulik, T. 2017, *MNRAS*, 464, L36, doi: [10.1093/mnrasl/slw177](https://doi.org/10.1093/mnrasl/slw177)
- Babak, S., Baker, J. G., Benacquista, M. J., et al. 2010, *Classical and Quantum Gravity*, 27, 084009, doi: [10.1088/0264-9381/27/8/084009](https://doi.org/10.1088/0264-9381/27/8/084009)
- Babak, S., Caprini, C., Figueroa, D. G., et al. 2023, *JCAP*, 2023, 034, doi: [10.1088/1475-7516/2023/08/034](https://doi.org/10.1088/1475-7516/2023/08/034)
- Baghi, Q. 2022, arXiv e-prints, arXiv:2204.12142, doi: [10.48550/arXiv.2204.12142](https://doi.org/10.48550/arXiv.2204.12142)
- Baker, J., Bellovary, J., Bender, P. L., et al. 2019, arXiv e-prints, arXiv:1907.06482, <https://arxiv.org/abs/1907.06482>
- Banerjee, S. 2017, *MNRAS*, 467, 524, doi: [10.1093/mnras/stw3392](https://doi.org/10.1093/mnras/stw3392)
- Banerjee, S., Baumgardt, H., & Kroupa, P. 2010, *MNRAS*, 402, 371, doi: [10.1111/j.1365-2966.2009.15880.x](https://doi.org/10.1111/j.1365-2966.2009.15880.x)
- Bartos, I., Kocsis, B., Haiman, Z., & Márka, S. 2017, *ApJ*, 835, 165, doi: [10.3847/1538-4357/835/2/165](https://doi.org/10.3847/1538-4357/835/2/165)
- Bassan, M. 2014, *Advanced interferometers and the search for gravitational waves: Lectures from the first VESF school on advanced detectors for Gravitational Waves* (Springer)

- Belczynski, K., Holz, D. E., Bulik, T., & O’Shaughnessy, R. 2016, *Nature*, 534, 512, doi: [10.1038/nature18322](https://doi.org/10.1038/nature18322)
- Belczynski, K., Kalogera, V., & Bulik, T. 2002, *ApJ*, 572, 407, doi: [10.1086/340304](https://doi.org/10.1086/340304)
- Bethe, H. A., & Brown, G. E. 1998, *ApJ*, 506, 780, doi: [10.1086/306265](https://doi.org/10.1086/306265)
- Bouffanais, Y., Mapelli, M., Santoliquido, F., et al. 2021, *MNRAS*, 507, 5224, doi: [10.1093/mnras/stab2438](https://doi.org/10.1093/mnras/stab2438)
- Breivik, K., Rodriguez, C. L., Larson, S. L., Kalogera, V., & Rasio, F. A. 2016, *ApJL*, 830, L18, doi: [10.3847/2041-8205/830/1/L18](https://doi.org/10.3847/2041-8205/830/1/L18)
- Chan, M. L., Messenger, C., Heng, I. S., & Hendry, M. 2018, *PhRvD*, 97, 123014, doi: [10.1103/PhysRevD.97.123014](https://doi.org/10.1103/PhysRevD.97.123014)
- Chen, N., Ni, Y., Holgado, A. M., et al. 2022, *MNRAS*, 514, 2220, doi: [10.1093/mnras/stac1432](https://doi.org/10.1093/mnras/stac1432)
- Colpi, M., Danzmann, K., Hewitson, M., et al. 2024, LISA Definition Study Report. <https://arxiv.org/abs/2402.07571>
- Croton, D. J. 2013, *PASA*, 30, e052, doi: [10.1017/pasa.2013.31](https://doi.org/10.1017/pasa.2013.31)
- Cutler, C., Berti, E., Holley-Bockelmann, K., et al. 2019, *Bulletin of the American Astronomical Society*, 51, 109, doi: [10.48550/arXiv.1903.04069](https://doi.org/10.48550/arXiv.1903.04069)
- de Mink, S. E., & Mandel, I. 2016, *MNRAS*, 460, 3545, doi: [10.1093/mnras/stw1219](https://doi.org/10.1093/mnras/stw1219)
- Digman, M. C., & Cornish, N. J. 2023, *Physical Review D*, 108, doi: [10.1103/physrevd.108.023022](https://doi.org/10.1103/physrevd.108.023022)
- Ford, K. E. S., & McKernan, B. 2022, *MNRAS*, 517, 5827, doi: [10.1093/mnras/stac2861](https://doi.org/10.1093/mnras/stac2861)
- Fryer, C. L., Belczynski, K., Wiktorowicz, G., et al. 2012, *ApJ*, 749, 91, doi: [10.1088/0004-637X/749/1/91](https://doi.org/10.1088/0004-637X/749/1/91)
- Gerosa, D., Ma, S., Wong, K. W. K., et al. 2019, *PhRvD*, 99, 103004, doi: [10.1103/PhysRevD.99.103004](https://doi.org/10.1103/PhysRevD.99.103004)
- Giacobbo, N., Mapelli, M., & Spera, M. 2018, *MNRAS*, 474, 2959, doi: [10.1093/mnras/stx2933](https://doi.org/10.1093/mnras/stx2933)
- Hinshaw, G., Larson, D., Komatsu, E., et al. 2013, *ApJS*, 208, 19, doi: [10.1088/0067-0049/208/2/19](https://doi.org/10.1088/0067-0049/208/2/19)
- Hobbs, G., Lorimer, D. R., Lyne, A. G., & Kramer, M. 2005, *MNRAS*, 360, 974, doi: [10.1111/j.1365-2966.2005.09087.x](https://doi.org/10.1111/j.1365-2966.2005.09087.x)
- Hurley, J. R., Pols, O. R., & Tout, C. A. 2000, *MNRAS*, 315, 543, doi: [10.1046/j.1365-8711.2000.03426.x](https://doi.org/10.1046/j.1365-8711.2000.03426.x)
- Hurley, J. R., Tout, C. A., & Pols, O. R. 2002, *MNRAS*, 329, 897, doi: [10.1046/j.1365-8711.2002.05038.x](https://doi.org/10.1046/j.1365-8711.2002.05038.x)
- Jani, K., Shoemaker, D., & Cutler, C. 2020, *Nature Astronomy*, 4, 260, doi: [10.1038/s41550-019-0932-7](https://doi.org/10.1038/s41550-019-0932-7)
- Korol, V., Rossi, E. M., Groot, P. J., et al. 2017, *Monthly Notices of the Royal Astronomical Society*, 470, 1894, doi: [10.1093/mnras/stx1285](https://doi.org/10.1093/mnras/stx1285)
- Kruckow, M. U., Tauris, T. M., Langer, N., Kramer, M., & Izzard, R. G. 2018, *MNRAS*, 481, 1908, doi: [10.1093/mnras/sty2190](https://doi.org/10.1093/mnras/sty2190)
- Kyutoku, K., & Seto, N. 2016, *MNRAS*, 462, 2177, doi: [10.1093/mnras/stw1767](https://doi.org/10.1093/mnras/stw1767)
- Lackeos, K., Littenberg, T. B., Cornish, N. J., & Thorpe, J. I. 2023, *Astronomy & Astrophysics*, 678, A123, doi: [10.1051/0004-6361/202347222](https://doi.org/10.1051/0004-6361/202347222)
- Lamberts, A., Blunt, S., Littenberg, T. B., et al. 2019, *MNRAS*, 490, 5888, doi: [10.1093/mnras/stz2834](https://doi.org/10.1093/mnras/stz2834)
- Madau, P., & Fragos, T. 2017, *ApJ*, 840, 39, doi: [10.3847/1538-4357/aa6af9](https://doi.org/10.3847/1538-4357/aa6af9)
- Mapelli, M. 2016, *MNRAS*, 459, 3432, doi: [10.1093/mnras/stw869](https://doi.org/10.1093/mnras/stw869)
- Mapelli, M., Giacobbo, N., Ripamonti, E., & Spera, M. 2017, *MNRAS*, 472, 2422, doi: [10.1093/mnras/stx2123](https://doi.org/10.1093/mnras/stx2123)
- Marchant, P., Langer, N., Podsiadlowski, P., Tauris, T. M., & Moriya, T. J. 2016, *A&A*, 588, A50, doi: [10.1051/0004-6361/201628133](https://doi.org/10.1051/0004-6361/201628133)
- McKernan, B., Ford, K. E. S., Bellovary, J., et al. 2018, *ApJ*, 866, 66, doi: [10.3847/1538-4357/aadae5](https://doi.org/10.3847/1538-4357/aadae5)
- Mennekens, N., & Vanbeveren, D. 2014, *A&A*, 564, A134, doi: [10.1051/0004-6361/201322198](https://doi.org/10.1051/0004-6361/201322198)
- Portegies Zwart, S. F., & McMillan, S. L. W. 2000, *ApJL*, 528, L17, doi: [10.1086/312422](https://doi.org/10.1086/312422)
- Randall, L., & Xianyu, Z.-Z. 2021, *The Astrophysical Journal*, 914, 75, doi: [10.3847/1538-4357/abfd2c](https://doi.org/10.3847/1538-4357/abfd2c)
- Ranjan, S., Jani, K., Nitz, A. H., Holley-Bockelmann, K., & Cutler, C. 2024, arXiv e-prints, arXiv:2406.11926, doi: [10.48550/arXiv.2406.11926](https://doi.org/10.48550/arXiv.2406.11926)
- Robson, T., Cornish, N. J., & Liu, C. 2019, *Classical and Quantum Gravity*, 36, 105011, doi: [10.1088/1361-6382/ab1101](https://doi.org/10.1088/1361-6382/ab1101)
- Rodriguez, C. L., Chatterjee, S., & Rasio, F. A. 2016, *PhRvD*, 93, 084029, doi: [10.1103/PhysRevD.93.084029](https://doi.org/10.1103/PhysRevD.93.084029)
- Rodriguez, C. L., Kremer, K., Chatterjee, S., et al. 2021, *Research Notes of the American Astronomical Society*, 5, 19, doi: [10.3847/2515-5172/abdf54](https://doi.org/10.3847/2515-5172/abdf54)
- Rodriguez, C. L., Morscher, M., Pattabiraman, B., et al. 2015, *PhRvL*, 115, 051101, doi: [10.1103/PhysRevLett.115.051101](https://doi.org/10.1103/PhysRevLett.115.051101)
- Sesana, A. 2016, *PhRvL*, 116, 231102, doi: [10.1103/PhysRevLett.116.231102](https://doi.org/10.1103/PhysRevLett.116.231102)
- Sesana, A. 2017, in *Journal of Physics Conference Series*, Vol. 840, *Journal of Physics Conference Series (IOP)*, 012018, doi: [10.1088/1742-6596/840/1/012018](https://doi.org/10.1088/1742-6596/840/1/012018)
- Spera, M., Mapelli, M., & Bressan, A. 2015, *MNRAS*, 451, 4086, doi: [10.1093/mnras/stv1161](https://doi.org/10.1093/mnras/stv1161)
- Spera, M., Mapelli, M., Giacobbo, N., et al. 2019, *MNRAS*, 485, 889, doi: [10.1093/mnras/stz359](https://doi.org/10.1093/mnras/stz359)

- Springel, V. 2010, MNRAS, 401, 791,
doi: [10.1111/j.1365-2966.2009.15715.x](https://doi.org/10.1111/j.1365-2966.2009.15715.x)
- Stone, N. C., Metzger, B. D., & Haiman, Z. 2017, MNRAS, 464, 946, doi: [10.1093/mnras/stw2260](https://doi.org/10.1093/mnras/stw2260)
- Toubiana, A., Sberna, L., Caputo, A., et al. 2021, Physical Review Letters, 126, doi: [10.1103/physrevlett.126.101105](https://doi.org/10.1103/physrevlett.126.101105)
- van den Heuvel, E. P. J. 2019, IAU Symposium, 346, 1,
doi: [10.1017/S1743921319001315](https://doi.org/10.1017/S1743921319001315)
- Vitale, S. 2016, Physical Review Letters, 117,
doi: [10.1103/physrevlett.117.051102](https://doi.org/10.1103/physrevlett.117.051102)
- Vogelsberger, M., Genel, S., Springel, V., et al. 2014a,
MNRAS, 444, 1518, doi: [10.1093/mnras/stu1536](https://doi.org/10.1093/mnras/stu1536)
- . 2014b, Nature, 509, 177, doi: [10.1038/nature13316](https://doi.org/10.1038/nature13316)
- Zhao, Y., Lu, Y., Yan, C., Chen, Z., & Ni, W.-T. 2023,
MNRAS, 522, 2951, doi: [10.1093/mnras/stad1107](https://doi.org/10.1093/mnras/stad1107)
- Ziosi, B. M., Mapelli, M., Branchesi, M., & Tormen, G.
2014, MNRAS, 441, 3703, doi: [10.1093/mnras/stu824](https://doi.org/10.1093/mnras/stu824)